Micromachines **2015**, *6*, 544-553; doi:10.3390/mi6050544

OPEN ACCESS

micromachines

ISSN 2072-666X

www.mdpi.com/journal/micromachines

Article

Transferable Integrated Optical SU8 Devices: From Micronic Waveguides to 1D-Nanostructures

Nolwenn Huby [1,*], John Bigeon [1], Gwennaël Danion [1], Jean-Luc Duvail [2], Françis Gouttefangeas [3], Loïc Joanny [3] and Bruno Bêche [1]

[1] Institut de Physique de Rennes, Université de Rennes 1, CNRS UMR 6251, 35042 Rennes Cedex, France; E-Mails: john.bigeon@gmail.com (J.B.); gwennael.danion@gmail.com (G.D.); bruno.beche@univ-rennes1.fr (B.B.)

[2] Institut des Matériaux de Nantes Jean Rouxel, Université de Nantes, CNRS UMR 6502, 44322 Nantes, France; E-Mail: jean-luc.duvail@cnrs-imn.fr

[3] ScanMAT–CMEBA, University of Rennes 1, Campus de Beaulieu, 35042 Rennes Cedex, France; E-Mails: francis.gouttefangeas@univ-rennes1.fr (F.G.); loic.joanny@univ-rennes1.fr (L.J.)

* Author to whom correspondence should be addressed; E-Mail: nolwenn.huby@univ-rennes1.fr; Tel.: +33-22-323-6225; Fax: +33-22-323-6717.

Academic Editor: Arnaud Bertsch

Received: 26 March 2015 / Accepted: 21 April 2015 / Published: 23 April 2015

Abstract: We report on optical components for integrated optics applications at the micro- and nanoscale. Versatile shapes and dimensions are achievable due to the liquid phase processability of SU8 resist. On the one hand, by adjusting the UV-lithography process, waveguiding structures are patterned and released from their original substrate. They can be replaced on any other substrate and also immerged in liquid wherein they still show off efficient light confinement. On the other hand, filled and hollow 1D-nanostructures are achievable by the wetting template method. By exploiting the large range of available SU8 viscosities, nanowires of diameter ranging between 50 nm and 240 nm, as well as nanotubes of controllable wall thickness are presented. Optical injection, propagation, and coupling in such nanostructures are relevant for highly integrated devices.

Keywords: integrated photonics; 1D-nanostructures; optical coupling; transferable waveguide; UV-lithography; wetting template method

---

1. Introduction

Since the 1990s, polymer materials have been the subject of intensive research for integrated photonics applications, such as telecommunication or sensing [1]. Many reasons explain this interest; first the versatility of their chemical structure offers a large range of optical properties. In addition, their liquid phase processability enables large volume and low-cost production facilities. Those advantages contrast with glass optical fibers. Indeed, although these fibers are largely used for carrying optical information over long distances, they are not convenient for complex integrated circuitry. In addition to being fragile, glass fiber devices are prepared by quite expensive processes.

Passive components made of photo-sensitive resists were first developed with ridge waveguides that are the base components of integrated optics circuits. Here, for an efficient optical confinement of the electromagnetic wave, transparency, straight walls, and low surface roughness are some of the main criteria. Among the photosensitive polymer materials exploited for integrated photonics applications [2], SU8 resist appears as an appropriate candidate, as demonstrated by numerous works in the literature. Indeed, UV-Lithography process on SU8 is compatible with optical requirements (for instance, a refractive index of 1.56 at 670 nm) and propagation losses of few dB/cm [3,4]. Additional steps involving plasma treatments have been demonstrated for improving these propagation losses [5]. More complex passive SU8 structures have been realized, such as interferometric structures for thermal, pressure or biological sensors [6–8], microresonators [9–11], or optical accelerometers [12]. Regarding active SU8-based structures, the main strategy deals with the dispersion of dyes in the SU8 matrix leading to amplified emission of rare-earths [13] or rhodamine [14]. In all these examples of passive or active devices realization, the UV-lithography process is based on a few technological steps, resulting in the fast and low-cost realization of integrated circuits simple.

Regarding down-scaling, the dimensions of waveguiding structures, high aspect ratio nanostructures (nanowires and nanotubes) appear as appropriate candidates. Two approaches are mainly developed for their fabrication. The first one is based on lithographic processes, mainly e-beam lithography and scanning probe lithography, such as scanning electrochemical lithography [15], scanning near-field optical lithography [16], or nano-imprint strategies [17]. All these methods make it possible to elaborate nanowires directly onto the photonic chip. In addition to lithography processes, the electrospinning [18,19] and the wetting template methods [20,21] have been shown as an easy, low cost, and environmentally friendly techniques to elaborate organic nanowires. O'Carroll *et al.* have reported the realization of semi-conducting polyfluorene nanowires exhibiting the first optically pumped lasing effect [22] in organic nanowire.

Here, we report on SU8 micronic and sub-micronic transportable optical waveguides, fabricated by UV-lithography and the wetting template method, respectively. Both techniques exploit the fact that SU8 is available in several viscosities, enabling the access to a large range of shapes and aspect ratios. In the first part, we present the fabrication and the optical characterizations of waveguiding structures that can be released from the substrate after the lithography process. It enables the positioning of the waveguiding structures on any substrate, or their dispersion in liquid media. In the second part, focus is made on 1D-nanostructures, fabricated by the wetting template method. By choosing the appropriate SU8 viscosity for the membrane impregnation, a large range of dimensions of nanowires and

nanotubes is achievable. The light injection, propagation, and optical coupling between two 1D-nanostructures are also demonstrated.

2. Results and Discussions

2.1. Transportable SU8 Micronic Waveguiding Structures

UV-Photolithography is a powerful technique for the fabrication of waveguiding structures of various dimensions and shapes. One limitation lies in the fact that the obtained patterns are bound to the substrate and, thus, cannot be manipulated. By adjusting the lithography process, we show that the structures can be released from the substrate and then transferred to any other substrate or to liquid media. This is of fundamental interest for applications such as microgripp [23] or biosensing [24].

2.1.1. UV Lithography Process and Transfer to Hybrid Medium

A thermal 1.2 µm-high SiO_2 layer, acting as the lower cladding (n = 1.45 at 670 nm), is grown on top of the Si (100) substrate. A first baking (3 min at 95 °C) on a hot plate is performed to remove any oxygen contamination and to enhance SU8 adhesion. The SU8-2025 (viscosity of 4500 cSt) is then deposited by spin-coating at 2000 rpm. Before the exposure, a second baking treatment (2 min at 65 °C and 5 min at 95 °C) helps to remove the undesirable solvents. Then, after the patterning by UV-exposure for 60 s at λ = 365 nm with a mercury lamp delivering on the sample P = 5 mW/cm^2, the development step takes place during 80 s in SU8-developer (propylene glycol monomethyl ether acetate). Finally, a final baking (1 min at 65 °C and 3 min at 95 °C) takes place to cross-link the polymer. Such a process allows us to build structures up to 30 µm high. The last baking step of several hours in oven at 200 °C is here avoided. This is the key point to make the structures releasable. The wafer is then cleaved by applying pressure on the edge with a diamond tip. As presented on Figure 1a, the waveguiding structures are not cut together with the substrate while cleaving the wafer, making them accessible and releasable from the substrate. By catching them gently with a tweezers, they can be transferred onto any substrate. Figure 1b displays a scanning electron microcopy (SEM) image of a ridge waveguide positioned on two polydimethylsiloxane (PDMS) plots. The good mechanical stiffness of the SU8 resist enables to get a self-standing straight waveguide despite the absence of a substrate over a few millimeters.

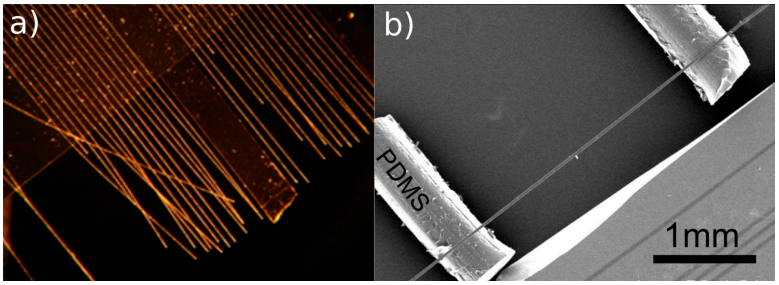

Figure 1. (**a**) Observation by optical microscope of micronic waveguiding structures after cleaving the wafer. Here, the lack of the final baking step prevents a strong adhesion between waveguide and SiO_2/Si wafer. As a result, the structures are not cleaved together with the wafer. (**b**) SEM image of a ridge waveguide, 10 µm wide, positioned by hand on two polydimethylsiloxane (PDMS) plots.

It is noteworthy that the choice of the SU8 viscosity is also key for this process and it must be high enough to ensure sufficient thickness. Indeed, by following the same process with the SU8-2002 (viscosity of 7.5 cSt) the fabricated structures are a few microns thick. While cleaving the wafer, the waveguiding structures are also cleaved, making them bound to the substrate.

2.1.2. Optical Characterizations of the Transportable Waveguiding Structures

The waveguiding structures were tested on a free-space microinjection bench with a laser diode centered at 670 nm. The light is collimated through a 20× objective and then focused onto the cross-section of the waveguide within a 40× objective. The transmitted light is collected with a second 40× objective and directed to a CCD camera to visualize the light confinement in the waveguiding structure. A top-view microscope enables the visualizing and positioning the sample.

Figure 2 presents optical microscope images during laser light injection in waveguiding structures positioned on two plots of PDMS in air (Figure 2a), and also immerged in silicon oil with a refractive index of 1.40 at 670 nm (Figure 2b). The PDMS has been chosen to minimize contact areas and for its refractive index (n = 1.41 at 670 mn [25]) that is compatible with optical confinement in SU8. Whatever the dimension of the waveguides, light propagation is effective and leads to a transmitted signal that is highlighted in the insets of Figure 2a,b, where light appears confined in the SU8 structure, both for air- and oil-surrounding media. From Figure 2a, optical losses can be estimated by the exponential decrease of the scattered light along the waveguide. A value of about 20 dB/cm is evaluated.

More complex waveguiding structures can be transferred following the process described above. Some tests were made with a disk light-reservoir that is a structure with a disk connected to a waveguide. Light was injected into the waveguide and propagated to the disk were light remains confined at the edges of the disk. The strong bend implies a large evanescent field in the surrounding medium, which can be exploited for evanescent coupling towards sub-micronic or micronic structures [26] or for species detection [16].

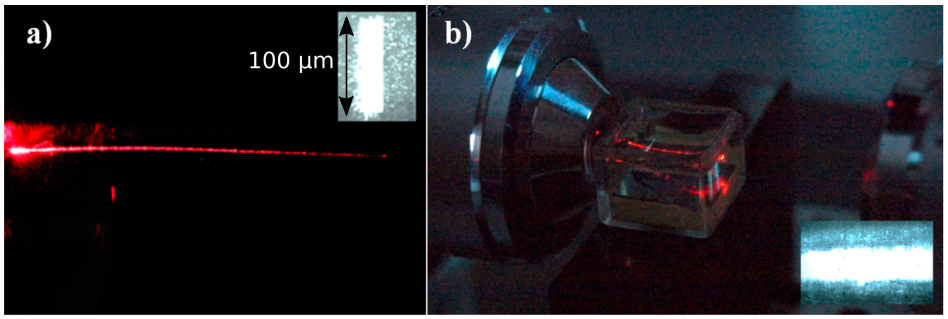

Figure 2. Top-view imaging of a 100 µm wide waveguide positioned on PDMS plots during laser light injection and propagation (λ = 670 nm), (**a**) in air, (**b**) immerged in silicon oil. The insets show the light confinement recorded on the CCD camera at the output of the waveguide.

2.2. SU8 1D-Nanostructures: From Nanowires to Nanotubes

The nanotubes and nanowires fabrication has been performed by a wetting template strategy. The description of the method is first presented, followed by structural characterizations of the 1D-nanostructures. Finally, optical injection and propagation in such nanostructures are demonstrated.

2.2.1. Fabrication by the Wetting Template Method

The wetting template method is based on the impregnation of a commercially available 60-µm thick alumina porous membrane (anodized aluminum oxide, AAO) with the SU8 photoresist, as described in Figure 3. After diffusion and evaporation of the solvent, the reticulation of the SU8 is performed under a UV lamp at λ = 365 nm. Then, the selective dissolution of the membrane takes place in a bath of either H_3PO_4 or NaOH during 12 h. Finally, the sample is rinsed in deionized water. The dispersion of the nanostructures is performed in an appropriate solvent with low surface tension, such as isopropanol (γ = 21.8 N/m). This is a key-step for the integration of NTs (nanotubes) as individual building-blocks in order to study their wave-guiding properties and to further design optical devices.

Energy dispersive X-ray spectroscopy (EDS) measurements have been performed before and after the membrane dissolution in NaOH in order to control its efficient removal. Both analyses are displayed in Figure 3. After dissolution, the aluminum signal has disappeared whereas the carbon one dominates the composition of the sample, validating the process. The weak signal at 1.04 keV is attributed to residual sodium from the membrane dissolution in NaOH.

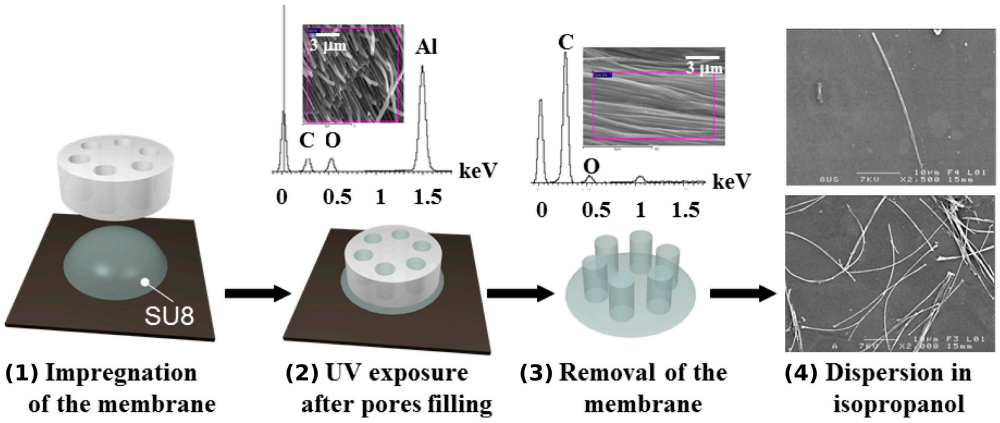

Figure 3. Illustration of the different steps of fabrication of organic nanostructures. (**1**) Deposition of the membrane on a drop of SU8 photoresist for membrane impregnation. EDS analysis are shown before (**2**) and after (**3**) removal of the membrane. (**4**) SEM images after dispersion by sonication in isopropanol and drop casting on a wafer.

The impregnation of the nanopores of the membrane is based on the surface tension difference between the membrane and the SU8 solvent, which ensures the wetting of the membrane. By modification of the SU8 viscosity, the solvent surface tension is also modified enabling the variation of the film thickness deposited along the nanopores walls. Impregnation of AAO membrane (reference *Whatman* supplied by Fisher Scientific) with nanopores diameter of 240 nm for different SU8 viscosities were performed. Figure 4a–c displays the SEM images of the obtained nanostructures for respective SU8 viscosities of 7.7 cSt (SU8-2002), 380 cSt (SU8-2010), and 4500 cSt (SU8-2025). For the lowest viscosity, nanotubes of an internal diameter of 120 nm are observed, while for the largest viscosity, nanowires are formed. It is emphasized that the good mechanical strength of the photoconverted SU8 allows the fabrication of very long and quite rigid nanostructures with a regular and cylindrical aspect along their length. The effect of the pore diameter for a fixed viscosity (7.7 cSt, SU8-2002) has been determined by wetting AAO membranes with various nanopores of diameters

(supplied by Synkera Technologies). Results displayed in Figure 4d–f show that the nanotubes wall decreases when the nanopores diameter decreases. In the extreme case of 55 nm nanopores diameter (Figure 4f), the nanotubes walls are too thin to enable a good mechanical strength, preventing the use of such nanotubes as building blocks.

These studies show that a large range of 1D-nanostructures dimensions is accessible by combining the wetting template method and the choice of the liquid resist.

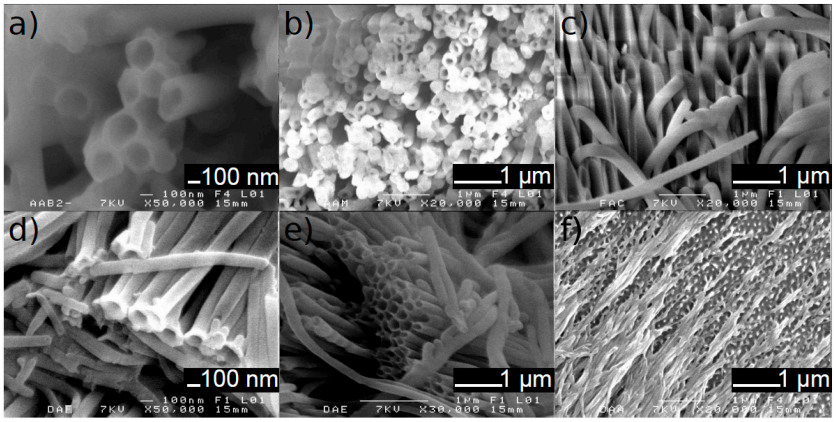

Figure 4. SEM images of the nanostructures obtained by the wetting template method. Case of fixed nanopores diameter of 240 nm with several SU8 viscosities: (**a**) nanotubes of internal diameter of about 120 nm (SU8-2002), (**b**) nanotubes of internal diameter of about 80 nm (SU8-2010), (**c**) nanowires (SU8-2025). By impregnating various nanopores diameter with SU8-2002, nanotubes of different dimensions are formed: (**d**) external and internal diameters of 150 nm and 70 nm respectively; (**e**) external and internal diameters of 100 nm and 50 nm, respectively; (**f**) case of nanopores of 55nm results in very flexible and wrapped nanostructures with a poor mechanical stiffness.

2.2.2. Optical Coupling and Propagation in 1D-Nanostructures

Relevant control of light injection in sub-micronic structures is a key-point for investigating sub-micronic waveguiding phenomena. The main conventional method is the evanescent coupling within stretched nanofibers [27]. Despite efficient optical coupling, this method presents some inconveniences, such as a subsequent length of coupling and a lack of control of the incident light intensity. Recently, we proposed a direct injection method based on optical fibers with submicronic radius of curvature. This method allows validating the efficient propagation in nanotubes with internal and external diameters of 120 nm and 240 nm, respectively. In addition, the attenuation coefficients were evaluated in these SU8 nanotubes by a cut-back method, adapted to submicronic structures and value of 1.25 dB/mm, was measured [28]. Since then, we have validated the injection and the propagation in nanotubes of different internal and external diameters accessible with the wetting template method described above.

Another coupling method developed in our group is based on the high evanescent field inherently surrounding sub-micronic structures. It has been exploited for coupling two waveguiding structures or for excitation of fluorescent labels [29]. Figure 5a,b present light injection and propagation along two SU8 nanotubes of 240 nm and 120 nm external and internal diameters respectively: light is injected

from a microlensed fiber into the nanotube located on the edge of the wafer, at the left side of the optical microscope image. Once aligned, and under light injection (λ = 675 nm), a spot at the output facet of both nanotube attests the effective injection, propagation, and coupling between the two adjacent nanotubes. These spots are highlighted on Figure 5b by the two circles. By imaging in 3D these propagative spot, it is shown that the intensity is decreased by a factor of ten. This decrease is attributed to the evanescent coupling and to the propagation losses along the longer nanotube.

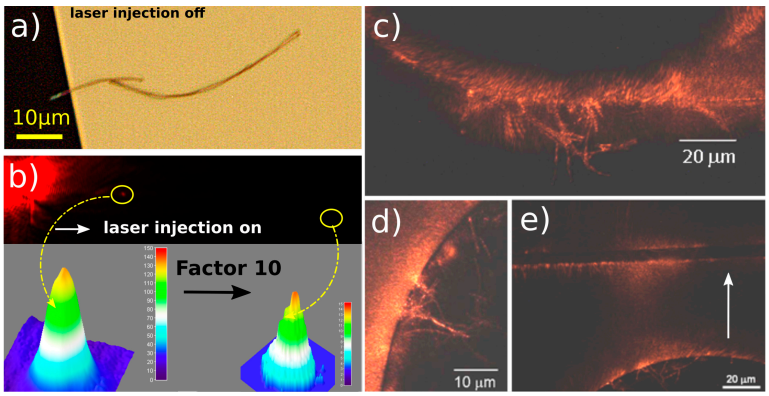

Figure 5. Evanescent coupling between SU8 micro- and nano-structures. (**a**) Top-view of a single nanotube positioned close to a second one. (**b**) Corresponding image during laser injection. The propagation along the first nanotube and the coupling and propagation into the second one are attested by the light spots at the end of the NTs, these being highlighted by the two circles. (**c**) Scheme of the configuration of optical coupling between SU8 microdisk and nanostructures and corresponding top-view images during light injection: area (1) coupling between nanotubes positioned at the surface of the SiO2/Si wafer; area (2) coupling with NTs localized on top of the disk; area (3) coupling from a disk-reservoir (where light is injected) to a rib waveguide through propagation along successive NTs. The arrow indicated the direction of light propagation.

Another interesting optical coupling phenomenon is presented on Figure 5c when the nanotubes are positioned close to SU8 disk light-reservoir connected to a rib waveguide. These microstructures were previously fabricated by classical UV-lithography. When light is injected in the ridge waveguide, the light propagates towards the disk-reservoir where photons are confined at the surface of the disk and a strong evanescent field is expected in the air due to the curved shape. Indeed, in a curved waveguide the Gaussian beam axis shifts towards the outside of the bend and leads to an extended evanescent tail [30] in the air as low refractive index medium. Thus, the disk-reservoir geometry is particularly suitable for achieving an evanescent coupling between micro-and nanostructures. This extension of the evanescent tail can be characterized by the displacement d, which is approximated by the formula:

$$d = \frac{\pi^2 n_{eff}^2 w_0^4}{\lambda_0^2 R} \quad (1)$$

where n_{eff}, w_0, λ_0 and R are the optical effective refractive index of the mode, the spot size, the laser vacuum wavelength (670 nm), and the radius of curvature. The effective refractive index and the spot size (*i.e.*, the half width of the Gaussian at 1/e) are calculated by polarized semi-vectorial finite difference method (SVDM) [31]. As the NTs and NWs (nanowires) are predicted as single mode

(fundamental HE_{11} mode) by the theoretical approach [18], the fundamental TE (transverse electric) and TM (transverse magnetic) modes in the microstructures present the highest probability to excite the nansotructures. The displacement d has been calculated for these both fundamental modes for which w_0 = 2.2 µm and n_{eff} = 1.5589. Thus, for the microdisk-reservoir of interest here, *d* is estimated about 6 microns. In other words, an efficient coupling is expected for NWs and NTs located in the 6-µm area surrounding the disk-reservoir.

A micro-beam profiler is placed on top of the bench allowing far-field visualization and intensity measurements. Different coupling configurations (areas 1, 2, and 3) on the photonic chip are presented on Figure 5. Area 1 is a view of several NTs placed on the SiO_2 substrate in the vicinity of the disk edges. The light is launched at the right side into the waveguide linked to the disk-reservoir where the light circulates at the surface. Area 2 presents an efficient optical coupling occurring with NTs positioned on top of the SU8 microdisk. Finally, area 3 depicts the connection between a disk-reservoir and a ridge waveguide connected by NTs. On the image, focus is made on top of the microstructures, the NTs lying on the substrate are not visible, contrary to the ones placed on top of the disk. Light is injected in the disk and it propagates by evanescent coupling into the NTs in the vicinity of the disk. One can see that NTs placed at a distance much larger than the penetration depth propagate light until the top waveguide, highlighting an efficient coupling between nanotubes. The light propagation along the top-waveguide indicates that the evanescent coupling from the nanotubes to the top waveguide is also efficient.

3. Conclusions

It was shown that the SU8 resist is a powerful and versatile material for transferable integrated devices fabrication from micro- to nanoscale. First, SU8 micronic waveguides were fabricated and can be released from their substrate and positioned elsewhere, in particular in liquid media, where they still conserve effective optical confinement. Then, by exploiting the different viscosities of the SU8, 1D-nanostructures were fabricated by the wetting template method: nanowires of 240 nm diameter, as well as nanotubes of inner and outer diameter ranging between 50 and 240 nm showing off losses values of few dB/cm. It is noteworthy that the limitation of the wetting template method is here evidenced with nanopores of diameter below 55 nm. The coupling between two nanostructures, as well as the coupling between micro- and nanostructures, are promising results for highly integrated photonics devices.

Acknowledgments

The authors thank CNRS and Region Bretagne for financial support. ScanMAT-CMEBA thanks Région Bretagne and European Union for financial support (CPER-FEDER 2007-2014). The authors thank Anthony Carré for 3D-graphics assistance.

Author Contributions

Nolwenn. Huby, John Bigeon, Gwennaël Danion, Jean-Luc Duvail and Bruno Bêche participated in the fabrication and optical characterizations of the waveguiding structures. Françis Gouttefangeas and Loïc Joanny are in charge of scanning electron microscopy and EDS analysis.

Conflicts of Interest

The authors declare no conflict of interest.

References

1. Eldada, L.; Shacklette, L.W. Advances in Polymer Integrated Optics. *IEEE J. Sel. Top. Quant. Elect.* **2000**, *6*, 54–68.
2. Ma, H.; Jen, A.K.-Y.; Dalton, L.R. Polymer-Based Optical Waveguides: Materials, Processing, and Devices. *Adv. Mat.* **2002**, *14*, 1339–1365.
3. Bêche, B.; Pelletier, N.; Hierle, R.; Goullet, A.; Landesman, J.P.; Gaviot, E.; Zyss, J. Conception of Optical Integrated Circuits on Polymers. *Microelectron. J.* **2006**, *37*, 421–427.
4. Nordström, M.; Zauner, D.A.; Boisen, A.; Hübner, J. Single-Mode Waveguides with SU-8 Polymer Core and Cladding for MOEMS Applications. *J. Lightwave Technol.* **2007**, *25*, 1284–1289.
5. Airoudj, A.; Debarnot, D.; Bêche, B.; Boulard, B.; Poncin-Epaillard, F. Improvement of the optical transmission of polymer planar waveguide by plasma treatment. *Plasma Process. Polym.* **2008**, *5*, 275–288.
6. Pelletier, N.; Bêche, B.; Gaviot, E.; Camberlein, L.; Grossard, N.; Polet, F.; Zyss, J. Single-mode rib optical waveguides on SOG/SU-8 polymer and integrated Mach-Zehnder for designing thermal sensors. *IEEE Sens. J.* **2006**, *6*, 565–570.
7. Pelletier, N.; Bêche, B.; Tahani, N.; Zyss, J.; Camberlein, L.; Gaviot, E. SU-8 waveguiding interferometric micro-sensor for gage pressure measurement. *Sens. Actuators A Phys.* **2007**, *135*, 179–184.
8. Shew, B.Y.; Cheng, Y.C.; Tsai, Y.H. Monolithic SU-8 micro-interferometer for biochemical detections. *Sens. Actuators A Phys.* **2008**, *141*, 299–306.
9. Scheuer, J.; Yariv, A. Fabrication and characterization of low-loss polymeric waveguides and micro-resonators. *J. Eur. Opt. Soc. Rapid Publ.* **2006**, *1*, 06007.
10. Rabiei, P.; Steier, W.H.; Zhang, C.; Dalton, L.R. Polymer micro-ring filters and modulators. *J. Lightwave Technol.* **2002**, *20*, 1968–1975.
11. Zebda, A.; Camberlein, L.; Bêche, B.; Gaviot, E.; Duval, D.; Zyss, J.; Jézéquel, G.; Solal, F.; Godet, C. Spin coating and plasma process for 2.5D integrated photonics on multilayer polymers. *Thin Solid Film* **2008**, *516*, 8668–8674.
12. Llobera, A.; Seidemann, V.; Plaza, J.A.; Cadarso, V.J.; Büttgenbach, S. SU-8 optical accelerometer. *J. Microelectromech. Syst.* **2007**, *16*, 111–121.
13. Tsang, K.C.; Wong, C.-Y.; Pun, E.Y.B. Eu^{3+}-Doped Planar Optical Polymer Waveguide Amplifiers. *IEEE Photonics Technol. Lett.* **2010**, *22*, 1024–1026.
14. Venugopal Rao, S.; Bettiol, A.A.; Watt, F. Characterization of channel waveguides and tunable microlasers in SU8 doped with rhodamine B fabricated using proton beam writing. *J. Phys. D Appl. Phys*. **2008**, *41*, 192002.
15. Jang, S.-Y.; Marquez, M.; Sotzing, G.A. Rapid direct nanowriting of conductive polymer via electrochemical oxidative nanolithography. *J. Am. Chem. Soc*. **2004**, *126*, 9476–9477.

16. Riehn, R.; Charas, A.; Morgado, J.; Cacialli, F. Near-field optical lithography of a conjugated polymer. *Appl. Phys. Lett*. **2003**, *82*, 526.
17. Hu, Z.; Muls, B.; Gence, L.; Serban, D.A.; Hofkens, J.; Melinte, S.; Nysten, B.; Demoustier-Champagne, S.; Jonas, A.M. High throughput fabrication of organic nanowire devices with preferential internal alignement and improved performance. *Nano Lett*. **2007**, *7*, 3639–3644.
18. Di Benedetto, F.; Camposeo, A.; Pagliara, S.; Mele, E.; Persano, L.; Stabile, R.; Cingolani, R.; Pisignano, D. Patterning of light-emitting conjugated polymer nanofibers. *Nat. Nanotechnol*. **2008**, *3*, 614–619.
19. Fasano, V.; Polini, A.; Morello, G.; Moffa, M.; Camposeo, A.; Pisignano, D. Bright light emission and waveguiding in conjugated polymer nanofibers electrospun from organic salt added solutions. *Macromolecules* **2013**, *46*, 5935–5942.
20. De Gennes, P.G. Wetting: Statics and dynamics. *Rev. Modern Phys.* **1985**, *57*, 827–863.
21. Steinhart, M.; Wendorff, J.H.; Greiner, A.; Wehrspohn, R.B.; Nielsch, K.; Schilling, J.; Choi, J.; Gösele, U. Polymer Nanotubes by Wetting of Ordered Porous Templates. *Science* **2002**, *296*, 1997.
22. O'Carroll, D.; Lieberwirth, I.; Redmond, G. Microcavity effects and optically pumped lasing in single conjugated polymer nanowires. *Nat. Nanotech*. **2007**, *2*, 180–184.
23. Panepuccia, R.R.; Martinez, J.A. Novel SU-8 optical waveguide microgripper for simultaneous micromanipulation and optical detection. *J. Vac. Sci. Technol. B* **2008**, *26*, 2624–2627.
24. Yin, D.; Lunt, E.J.; Rudenko, M.I.; Deamer, D.W.; Hawkins, A.R.; Schmidt, H. Planar optofluidic chip for single particle detection, manipulation, and analysis. *Lab Chip* **2007**, *7*, 1171–1175.
25. Cai, Z.; Qiu, W.; Shao, G.; Wang, W. A new fabrication method for all-PDMS waveguides. *Sens. Actuators A Phys.* **2013**, *204*, 44–47.
26. Huby, N.; Duvail, J.-L.; Duval, D.; Pluchon, D.; Bêche, B. Light propagation in songlemode polymer nanotubes integrated on photonic circuits. *Appl. Phys. Lett.* **2011**, *99*, 113302.
27. Huang, K.; Yang, S.; Tong, L. Modeling of evanescent coupling between two parallel optical nanowires. *Appl. Opt.* **2007**, *46*, 1429–1434.
28. Bigeon, J.; Huby, N.; Duvail, J.-L.; Bêche, B. Injection and waveguiding properties in SU8 nanotubes for sub-wavelength regime propagation and nanophotonics integration. *Nanoscale* **2014**, *6*, 5309–5314.
29. Leosson, K.; Agnarsson, B. Integrated biophotonics with CYTOP. *Micromachines* **2012**, *3*, 114–125.
30. Nishihara, H.; Haruna, M.; Suhara, T. *Optical Integrated Circuits*; MacGrow-Hill Publishing Co: New York, NY, USA, 1989; p. 43.
31. Bêche, B.; Jouin, J.F.; Grossard, N.; Gaviot, E.; Toussaere, E.; Zyss, J. PC software for analysis of versatile integrated optical waveguides by polarised semi-vectorial finite difference method. *Sens. Actuators A Phys.* **2004**, *114*, 59–64.